Electronic Supplementary Material (ESI) for New Journal of Chemistry.

Supplementary Information

Functionalized D/A-A-D Quinolines for the Application in Solution-Processable p-Channel Organic Field-Effect Transistors

Anshika Anjali,[a] Sambit Kumar Lenka,[a] Predhanekar Mohamed Imran,[b] Nattamai S. P. Bhuvanesh,[c] Samuthira Nagarajan*[a]

[a.] *Organic Electronic Materials Division, Department of Chemistry, Central University of Tamil Nadu, Thiruvarur- 610 005, India, *Email: snagarajan@cutn.ac.in*

[b.] *Department of Chemistry, Islamiah College, Vaniyambadi - 635 752, India*

[c.] *Department of Chemistry, Texas A &M University, TX77842, USA*

Table of Contents

Photophysical Analysis

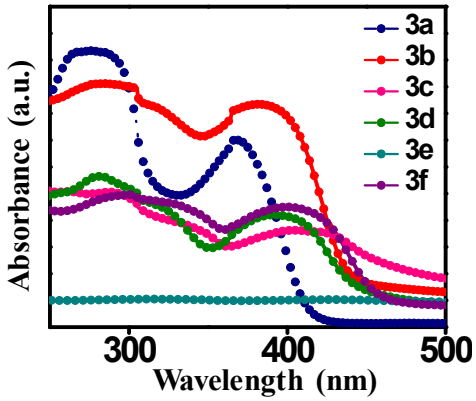

Figure S1. Film-state absorption spectra of compounds **3a-f**.

Thermal Analysis

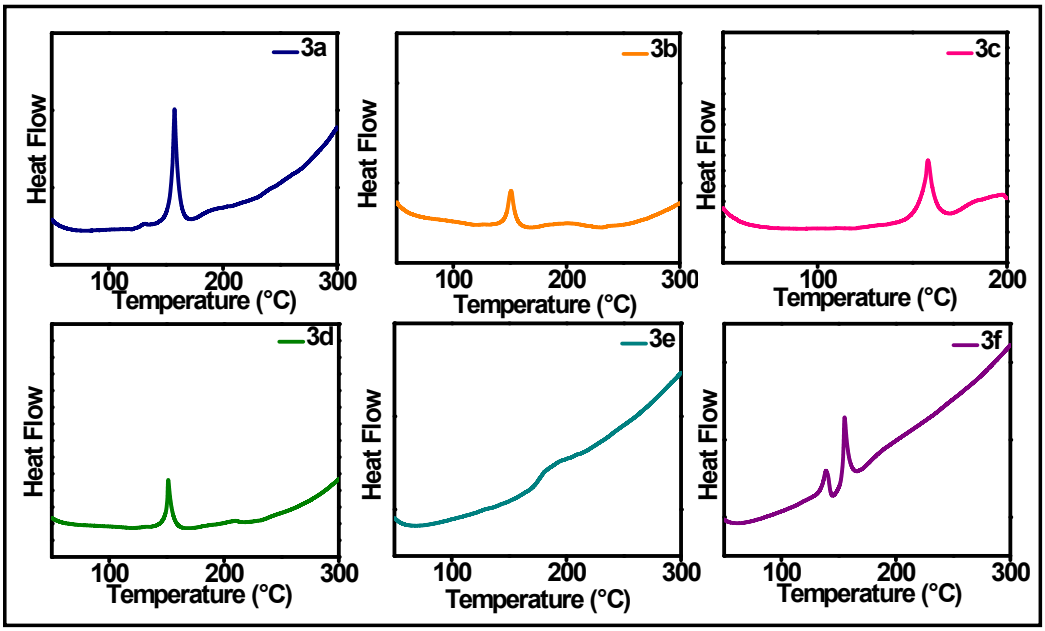

Figure S2. DSC thermogram of compounds **3a-f**.

Table S1. DSC data of compounds **3a-f**.

Comp.	T_m (°C)
3a	157.0
3b	151.0
3c	158.3
3d	151.4
3e	186.5
3f	154.6

Electrochemical Studies

(a)

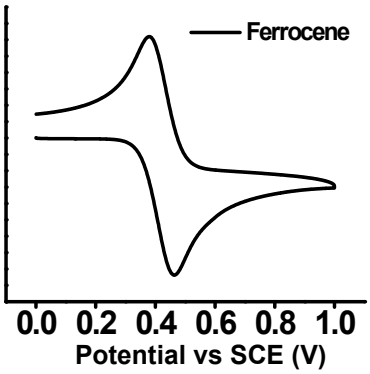

(b)

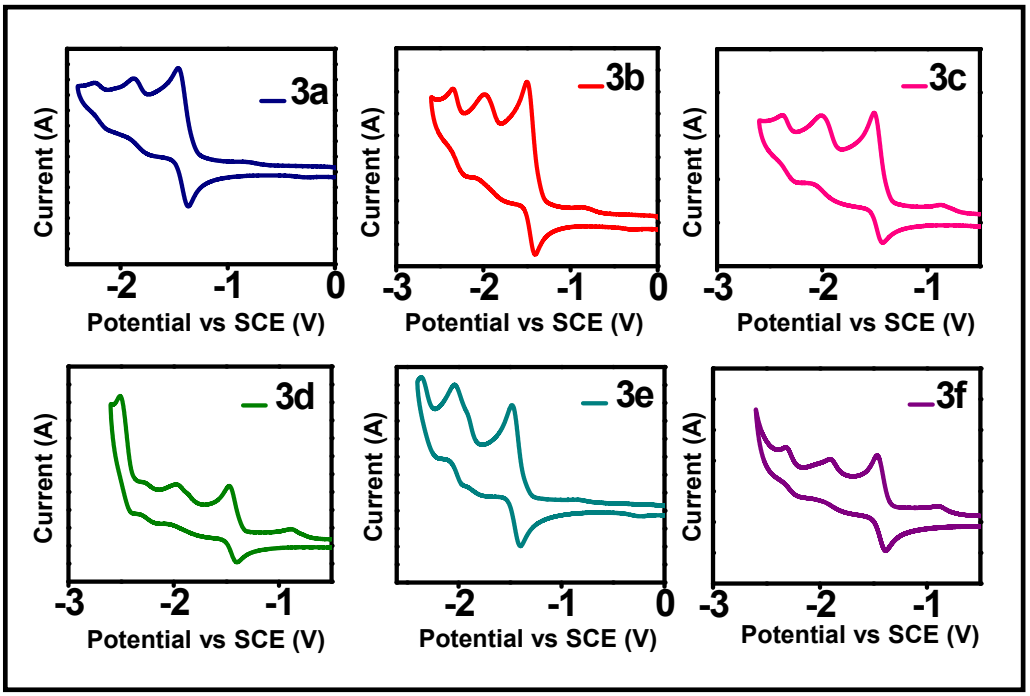

Figure S3. (a) Cyclic voltammogram of ferrocene, and (b) compounds **3a-f**.

Computational Studies

The geometrical parameters were used to compute the optimized structure (**Figure S4**) at the DFT- B3LYP level of theory and TD-SCF for spectral estimation theoretically using *Gaussian*. This optimized geometry was then used as input geometry for Density of State (DOS) calculations using *VASP (MedeA)* software. To involve solvent correction GGA-PBE basis set was used and the DOS graphs were obtained. The Fermi energy and band gaps were also computed along with the density and volume of the cell. All the molecules pertained to a simple orthorhombic system (**Table S4**). The Density of States calculated using the GGA-PBE basis set are visualized and presented as DOS graphs (**Figure S6).** The figure shows many Fermi levels for the occupied levels and the Fermi gaps are presented in **Table S3**.

The bandgap values are smaller for all the molecules suggesting good transportability of charge carriers. However, compounds **3d**, **3e**, and **3f** have relatively smaller values of bandgap which are in accordance with the experimental results. The Fermi gap is almost similar except for compound **3a**. While Fermi gaps represent the availability of space for the movement of electrons, the DOS represents the number of states which offer high space for the particle movements. From the DOS graphs, it can be seen that an occupied state in **3d** has a maximum value of around 6eV. This is probably due to the presence of F-atom which is highly electronegative and thus has a higher inductive effect over the other molecules. This type of substitution may affect the entire geometry and thus the nature of the molecule. It thus has the largest number of states for particle movement. It is also observed that the valence levels or the LUMO levels are more for this molecule. In contrast, compound **3b** has the least such states.

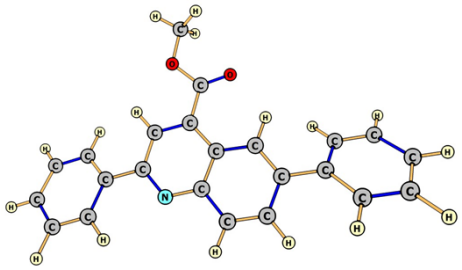

Figure S4. A general representation of compound **3a**.

These are the states where excited electrons may be promoted to account for the spectral and conducting properties of the molecule. The TDDFT calculations also show various states within the experimentally measured values. For compound **3b,** no plausible triplet state excitations and the highest theoretical values for Energy were observed.

Table S2. Electronic absorption behaviour of compounds **3a-f** by TD-DFT.

Comp. 3	Wavelength (nm)	Energy (eV)	Oscillator strength (f)	Electronic Transitions (eV)
a	414.2	2.993	0.000	S_{-1}-T_1
	360.5	3.439	0.000	S_0-T_2
b	430.1	2.882	0.000	S_o-T_1
	377.6	3.282	0.012	S_o-T_2
c	520.0	2.384	0.000	S_0-T_1
	379.3	3.268	0.523	S_0-S_1
d	406.2	3.052	0.340	S_0-S_1
	343.6	3.608	0.027	S_{-1}-S_2
e	431.2	2.875	0.000	S_{-3}-T_1
	381.7	3.248	0.000	S_{-5}-T_1
f	436.2	2.842	0.000	S_{-1}-T_1
	392.2	3.161	0.093	S_0-T_2

The MedeA was used to generate the PBC values from which the molecular packing was obtained. These values were used to build up the polycrystals of respective molecules. The packing distance and hopping values were predicted and are listed in **Table S3**. The hopping distances are indicated by lines in the respective packing as shown in **Figure S5**. The interatomic distances of the molecules were obtained considering the volume and space groups. The distance of interaction between H atom with O and N of the adjacent molecule to account for non-covalent interactions. While some inter-atomic distances were monitored and

measured below 10Aº, other hopping distances were calculated by the software. Compound **3b** with methoxy substituents at the end terminals resulted in close packing with low hopping distances. The compounds **3e** with biphenyl and **3f** with thiophene substituted at the sixth position of the quinolines resulted in the highest hopping distances and thus have less dense packing. Compound **3d** resulted in the least hopping distance values and thus resulted in dense packing(**Table S3**).

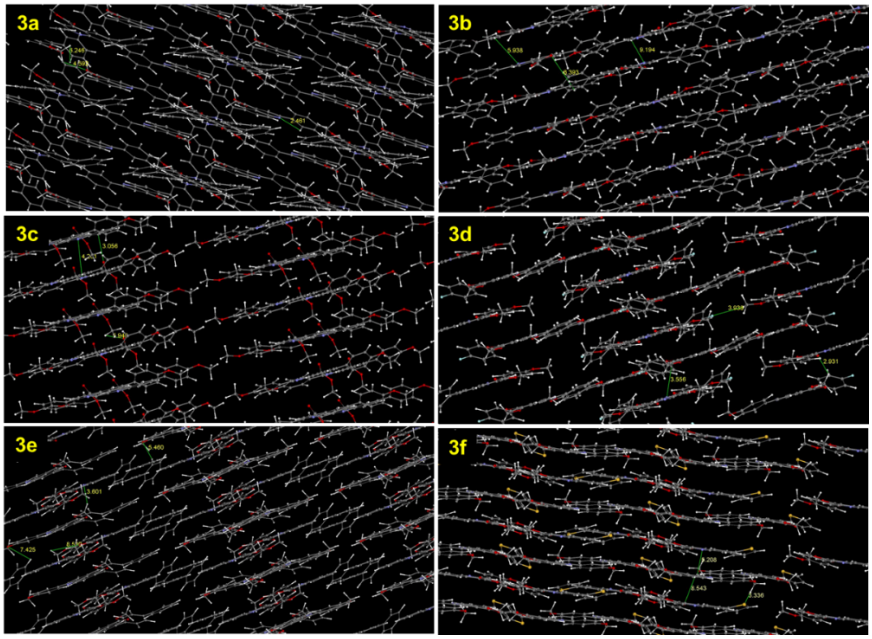

Figure S5. Molecular packing and hopping distance calculation from polycrystalline packing of compounds **3a-f**.

Table S3. Hopping distance and bandgap of compounds **3a-f**.

	Volume Å^3	Density mg/m^3	Hopping Distances(Å)	DOS band gap (eV) DFT GGA-PBE	PBC Unit
3a	1611.21	0.35	2.461 4.592 6.426	2.222	314
3b	1825.31	0.34	5.938 6.393 9.194	2.004	314
3c	2154.34	0.31	3.056 4.261 5.940	2.189	324
3d	1833.76	0.35	2.931 3.556 3.938	1.932	214
3e	2152.70	0.34	3.601 5.460 7.425	1.879	315
3f	1673.80	0.37	3.336 5.208 8.543	1.875	314

Table S4. Crystal and lattice structure parameters at ground level S_0.

	Type	Sides			Angle		
		A	**B**	**C**	**α**	**β**	**γ**
3a	Orthorhombic (**P21C**)	19.6	12.7	6.4	90	90	90
3b	Orthorhombic (PNA-21)	21.8	12.8	6.5	90	90	90
3c	Orthorhombic (**PC**)	23.9	10.6	8.4	90	90	90
3d	Orthorhombic (P21-C)	22.0	12.8	6.4	90	90	90
3e	Orthorhombic (**P21-C**)	26.1	12.7	6.4	90	90	90
3f	Orthorhombic	21.3	12.7	6.1	90	90	90

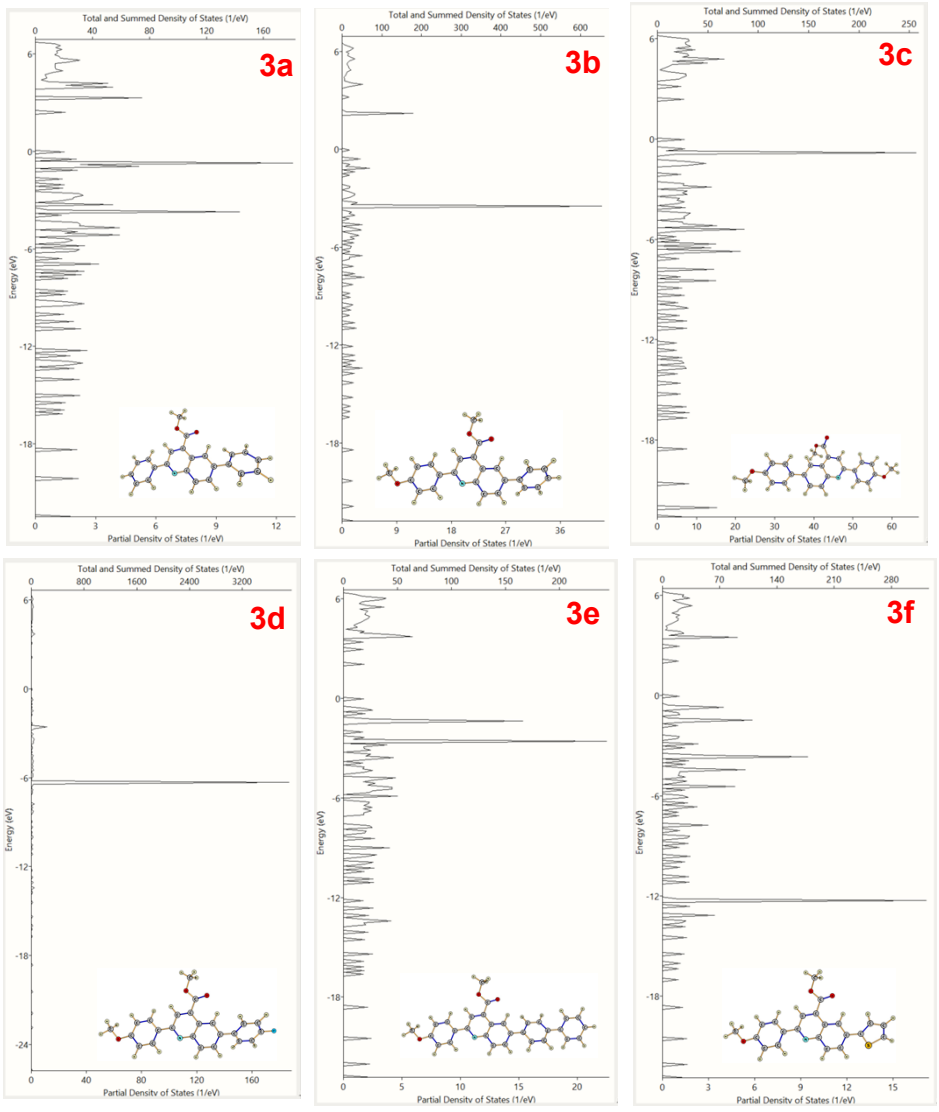

Figure S6. The density of States graphs of compounds **3a-f** (Inset is stabilized ground state structures).

Table S5. Crystal data and structure refinement for compounds 3a, 3d and, 3e .

Compound	**3a**	
Identification code for compound **3a**	2079814	
Empirical formula	C23 H17 N O2	
Formula weight	339.38	
Temperature	110.0 K	
Wavelength	1.54178 Å	
Crystal system	Monoclinic	
Space group	P 1 21/c 1	
Unit cell dimensions	a = 9.4119(3) Å	α= 90°.
	b = 16.8978(5) Å	β= 104.4160(10)°.
	c = 10.9784(4) Å	γ = 90°.
Volume	1691.03(10) $Å^3$	
Z	4	
Density (calculated)	1.333 Mg/m^3	
Absorption coefficient	0.676 mm^{-1}	
F(000)	712	
Crystal size	0.347 x 0.321 x 0.068 mm^3	
Theta range for data collection	4.851 to 70.141°.	
Index ranges	-11<=h<=11, -18<=k<=20, -13<=l<=13	
Reflections collected	23967	
Independent reflections	3214 [R(int) = 0.0448]	
Completeness to theta = 67.679°	99.7 %	
Absorption correction	Semi-empirical from equivalents	
Max. and min. transmission	0.4684 and 0.3081	
Refinement method	Full-matrix least-squares on F^2	
Data / restraints / parameters	3214 / 0 / 236	
Goodness-of-fit on F^2	1.060	
Final R indices [I>2sigma(I)]	R1 = 0.0557, wR2 = 0.1414	
R indices (all data)	R1 = 0.0577, wR2 = 0.1434	
Extinction coefficient	n/a	
Largest diff. peak and hole	0.636 and -0.279 $e.Å^{-3}$	
Compound	**3d**	
Identification code for compound 3d	2081459	
Empirical formula	C24 H18 F N O3	
Formula weight	387.39	
Temperature	110.0 K	
Wavelength	1.54178 Å	
Crystal system	Monoclinic	
Space group	P 1 21/c 1	
Unit cell dimensions	a = 9.7824(4) Å	α= 90°.
	b = 18.5157(7) Å	β= 113.429(2)°.
	0c = 11.0961(3) Å	γ = 90°.
Volume	1844.11(12) $Å^3$	
Z	4	
Density (calculated)	1.395 Mg/m^3	
Absorption coefficient	0.814 mm^{-1}	
F(000)	808	

Crystal size	0.562 x 0.074 x 0.038 mm^3
Theta range for data collection	4.776 to 70.108°.
Index ranges	-11<=h<=11, -22<=k<=22, -11<=l<=13
Reflections collected	14724
Independent reflections	3471 [R(int) = 0.0450]
Completeness to theta = 67.679°	99.2 %
Absorption correction	Semi-empirical from equivalents
Max. and min. transmission	0.4684 and 0.3827
Refinement method	Full-matrix least-squares on F^2
Data / restraints / parameters	3471 / 0 / 264
Goodness-of-fit on F^2	1.056
Final R indices [I>2sigma(I)]	R1 = 0.0458, wR2 = 0.1162
R indices (all data)	R1 = 0.0541, wR2 = 0.1208
Extinction coefficient	n/a
Largest diff. peak and hole	0.413 and -0.295 e.$Å^{-3}$

Compound	**3e**	
Identification code for compound **3e**	2095117	
Empirical formula	C30 H23 N O3	
Formula weight	445.49	
Temperature	110.0 K	
Wavelength	1.54178 Å	
Crystal system	Orthorhombic	
Space group	$P2_12_12_1$	
Unit cell dimensions	a = 13.8744(5) Å	α= 90°.
	b = 17.3267(6) Å	β= 90°.
	c = 27.3337(10) Å	γ = 90°.
Volume	6571.0(4) Å3	
Z	12	
Density (calculated)	1.351 Mg/m^3	
Absorption coefficient	0.693 mm-1	
F(000)	2808	
Crystal size	0.254 x 0.102 x 0.081 mm3	
Theta range for data collection	3.020 to 70.050°.	
Index ranges	-16<=h<=14, -21<=k<=21, -33<=l<=33	
Reflections collected	116183	
Independent reflections	12432 [R(int) = 0.0481]	
Completeness to theta = 67.679°	99.9 %	
Absorption correction	Semi-empirical from equivalents	
Max. and min. transmission	0.7533 and 0.6478	
Refinement method	Full-matrix least-squares on F2	
Data / restraints / parameters	12432 / 0 / 925	
Goodness-of-fit on F2	1.060	
Final R indices [I>2sigma(I)]	R1 = 0.0289, wR2 = 0.0756	
R indices (all data)	R1 = 0.0304, wR2 = 0.0766	
Absolute structure parameter	0.01(4)	
Extinction coefficient	n/a	
Largest diff. peak and hole	0.182 and -0.174 e.Å-3	

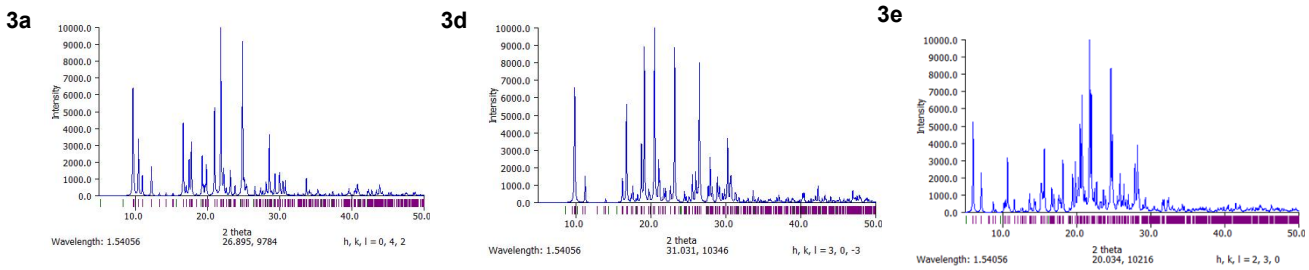

Figure S7. PIXRD spectra of compounds **3a, 3d,** and **3e**.

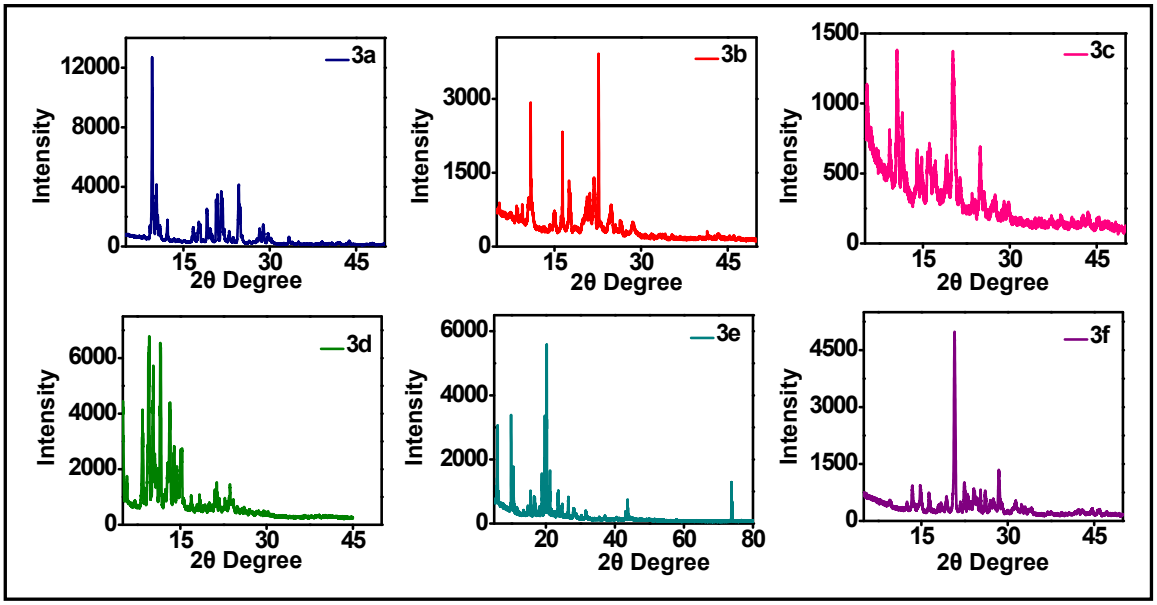

Figure S8. GIXRD spectra of compounds **3a-f**.

Schematic representation of fabricated OFET device

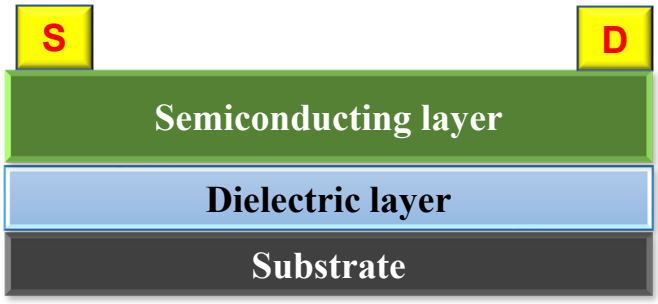

Figure S9. Schematics of the OFET device

The bottom gate-top contacts(BGTC) OFET devices were fabricated (**Figure S9**). The doped Si substrate was used as a gate electrode which was pre-cleaned by following the RCA cleaning procedure[i,ii] followed by a thermally grown SiO_2 layer as the dielectric layer. The semiconducting layers were then fabricated using spin-coating techniques to obtain uniform surface morphology with a concentration of 5 mg/ml and underwent post-annealing till 120 °C to eliminate the traps. Silver contacts were made for the source and drain terminals.

The mobility values were calculated from the saturation regime of the transfer curves by using the following equation[iii]

$\mu = 2L(Slope)^2/CW$

Where, W and L are the width of the channel and length, respectively, C is the capacitance of the SiO_2 dielectric layer per unit area.

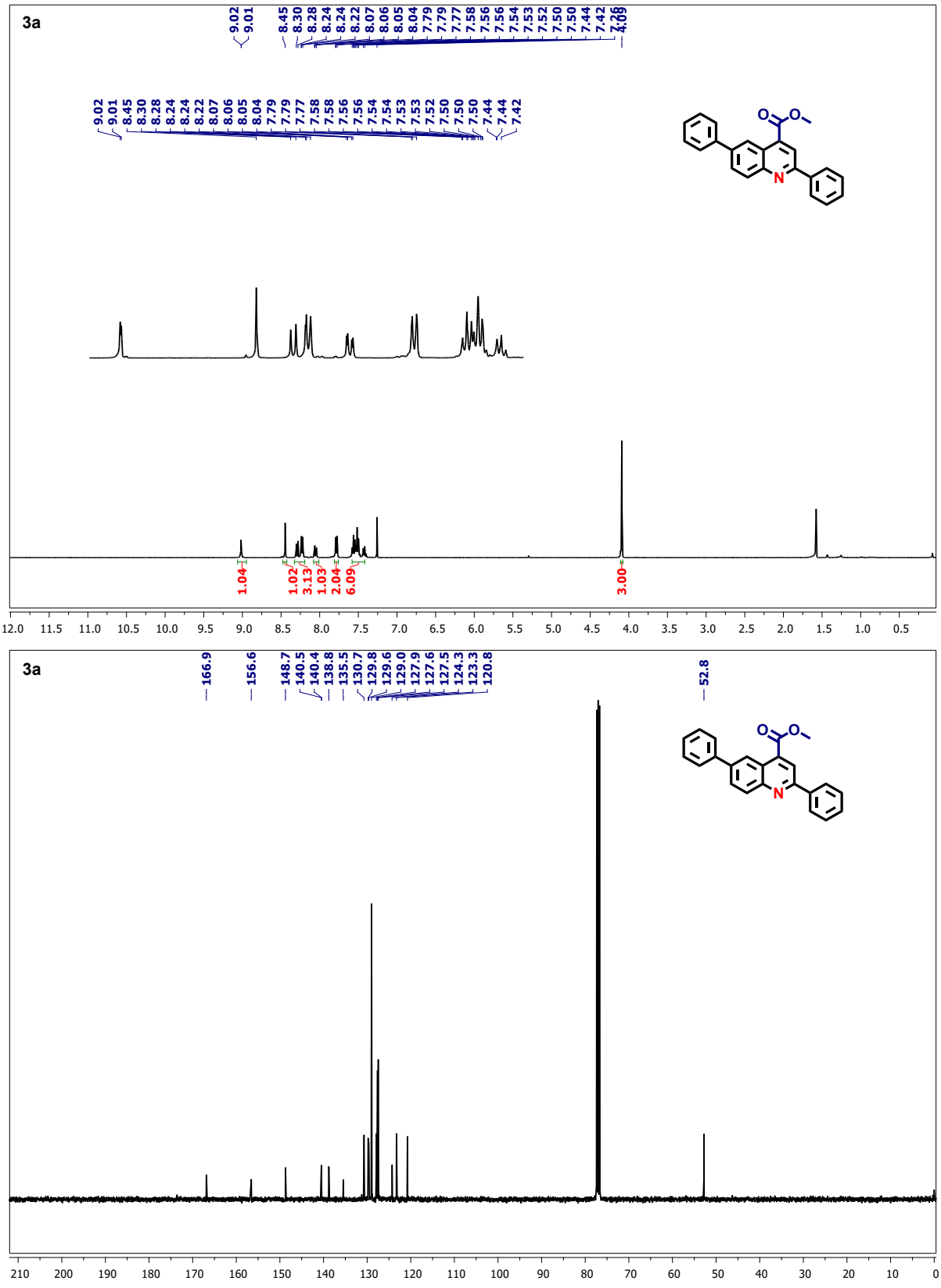

Figure S10. ^{1}H and ^{13}C NMR spectra of compound **3a**.

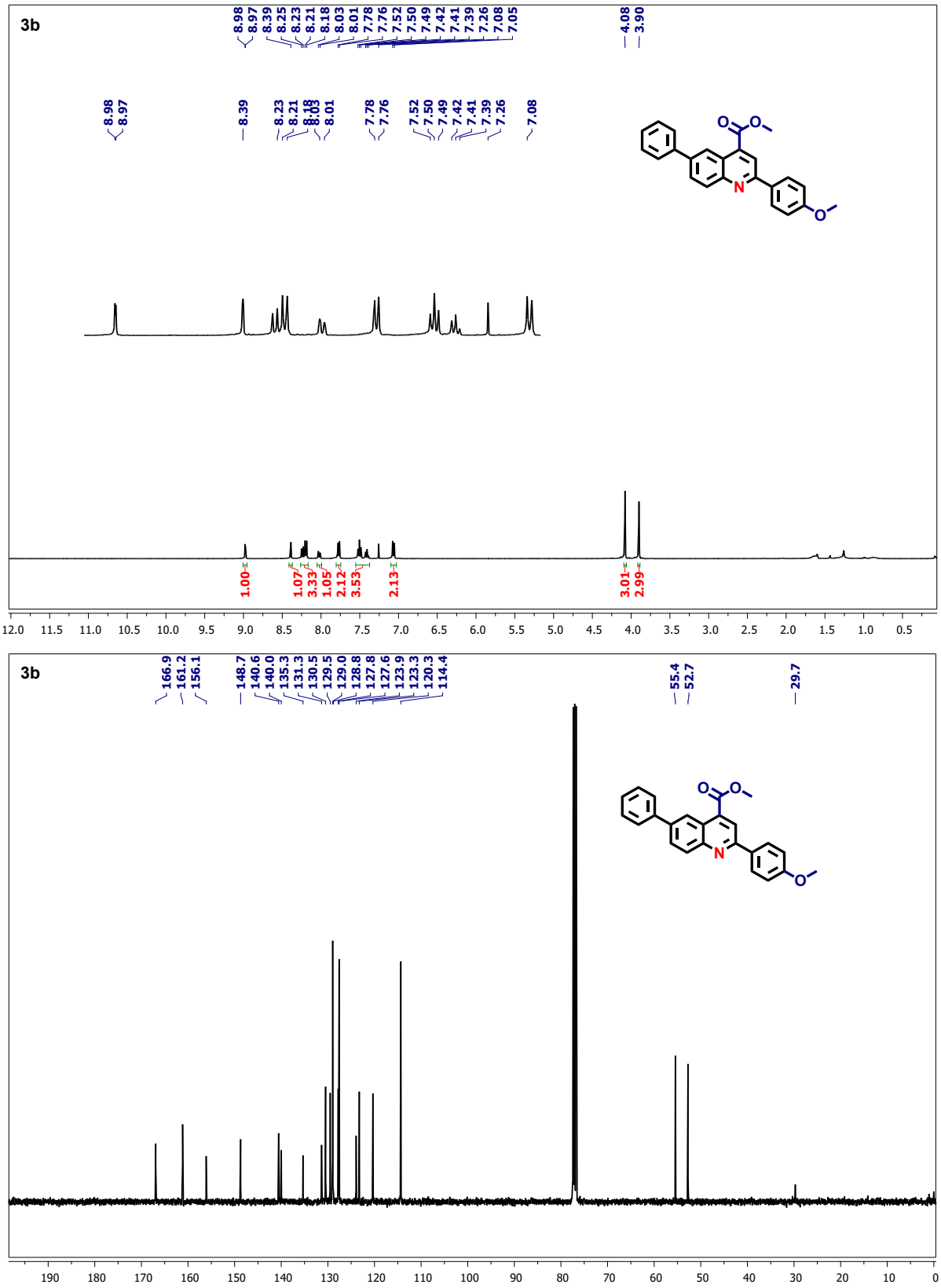

Figure S11. ^{1}H and ^{13}C NMR spectra of compound **3b**.

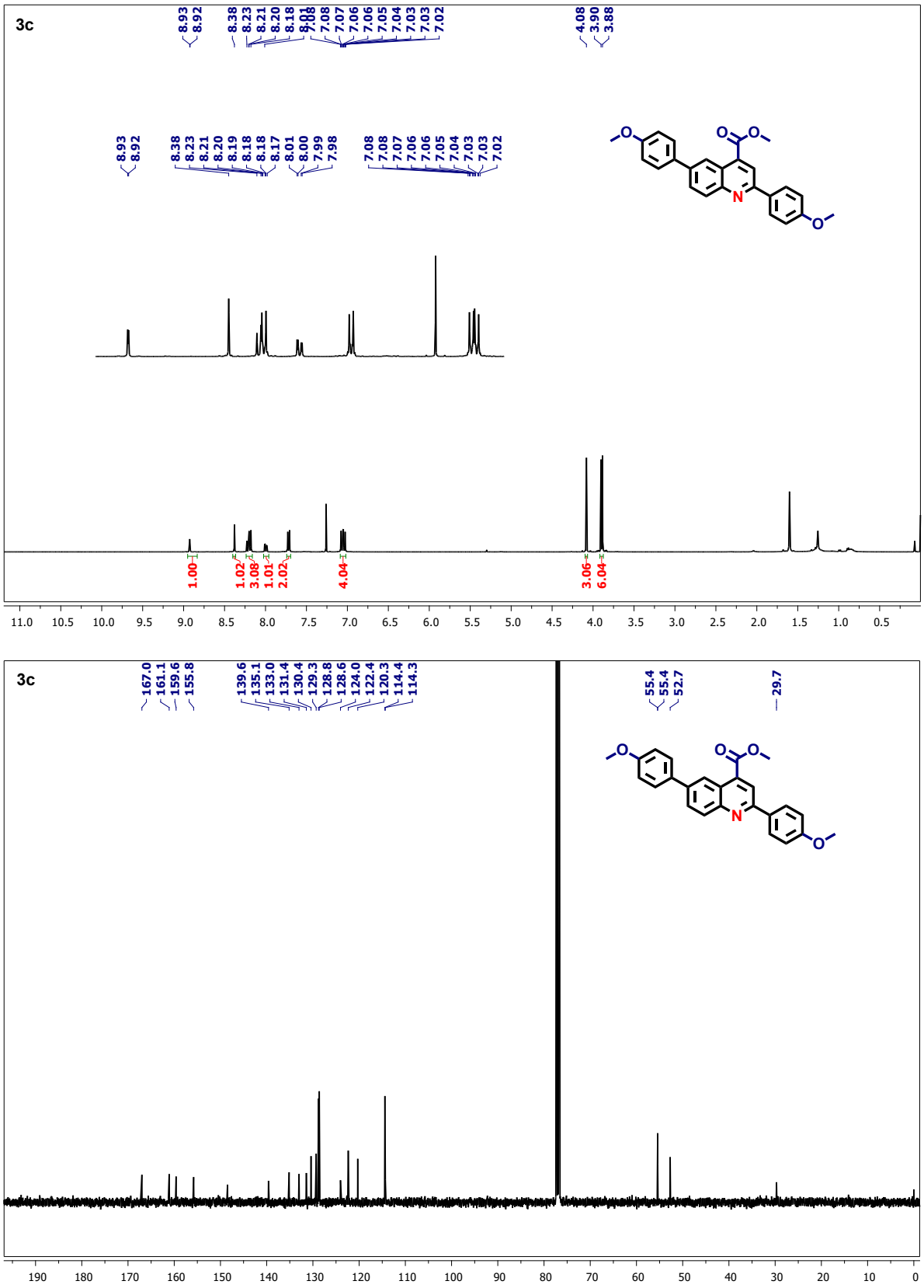

Figure S12. ^{1}H and ^{13}C NMR spectra of compound **3c**.

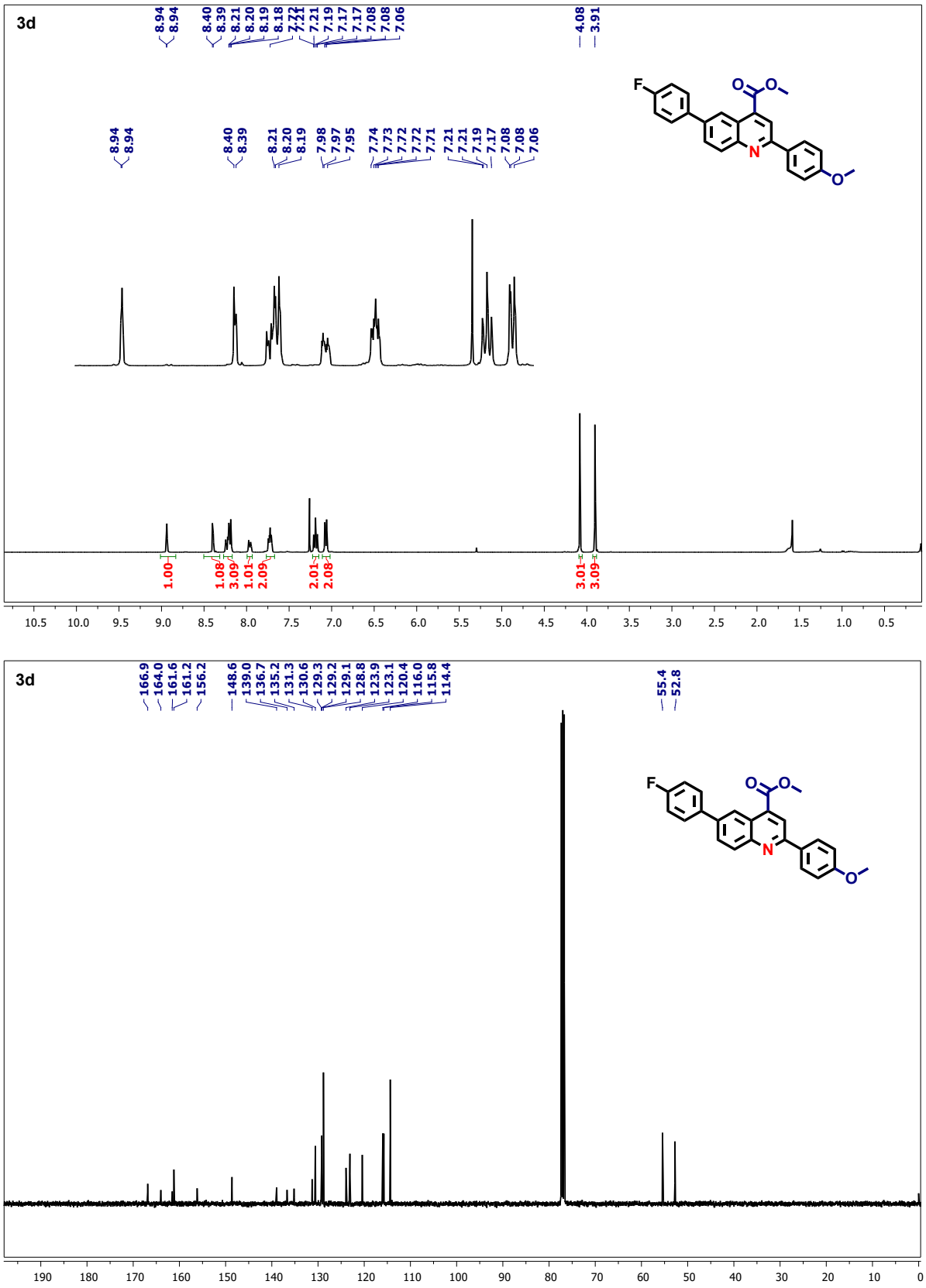

Figure S13. ^{1}H and ^{13}C NMR spectra of compound **3d**.

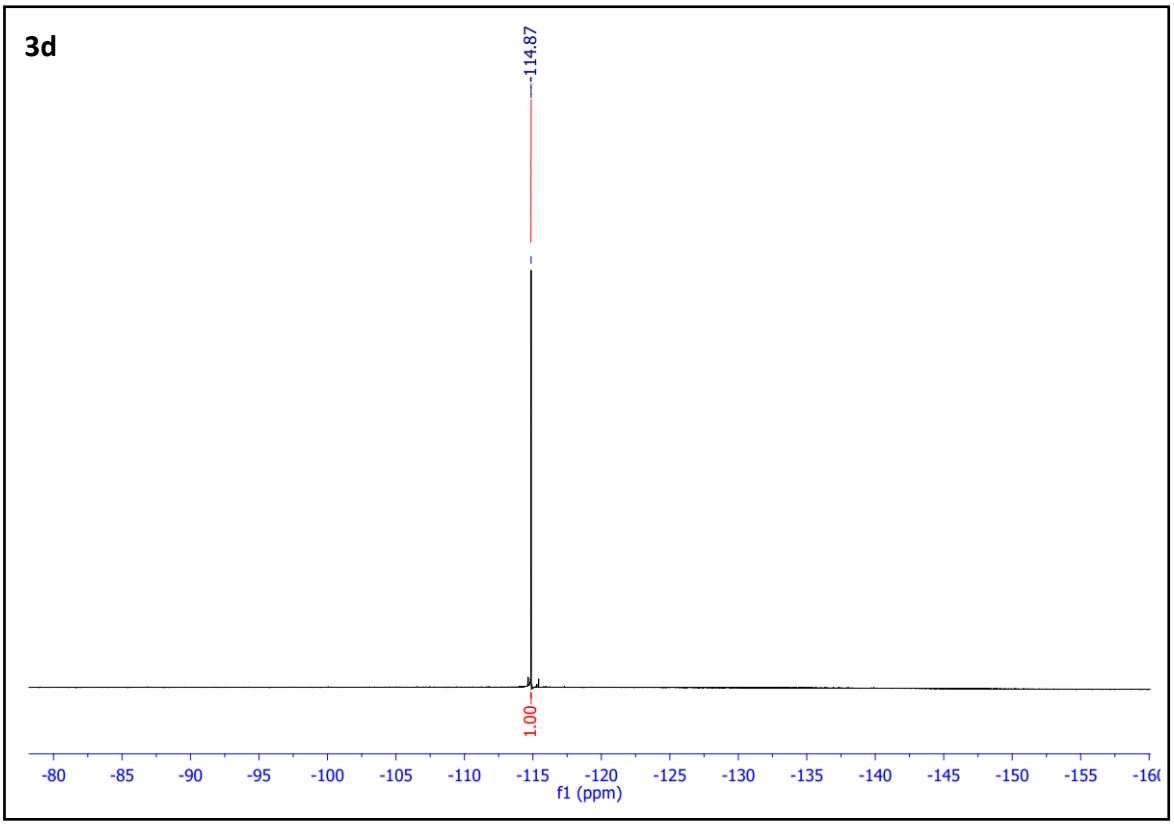

Figure S14. ^{19}F NMR spectrum of compound **3d**.

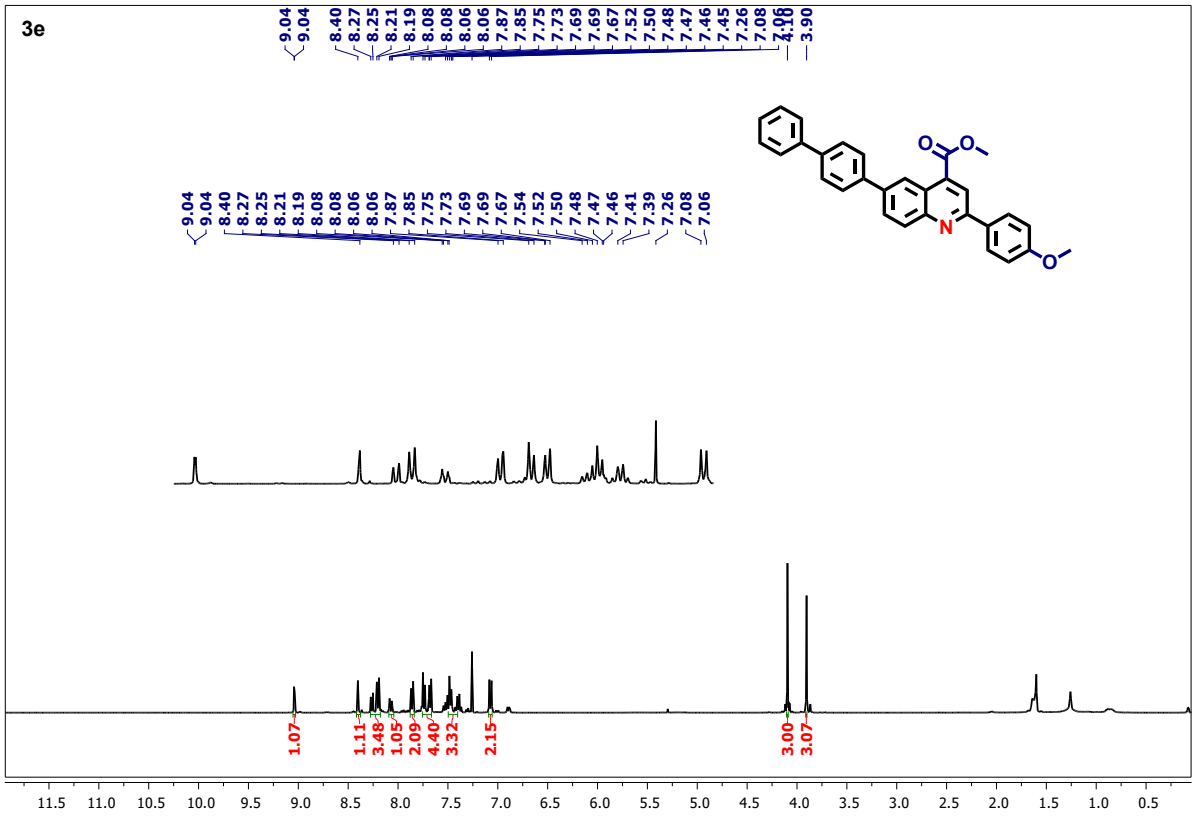

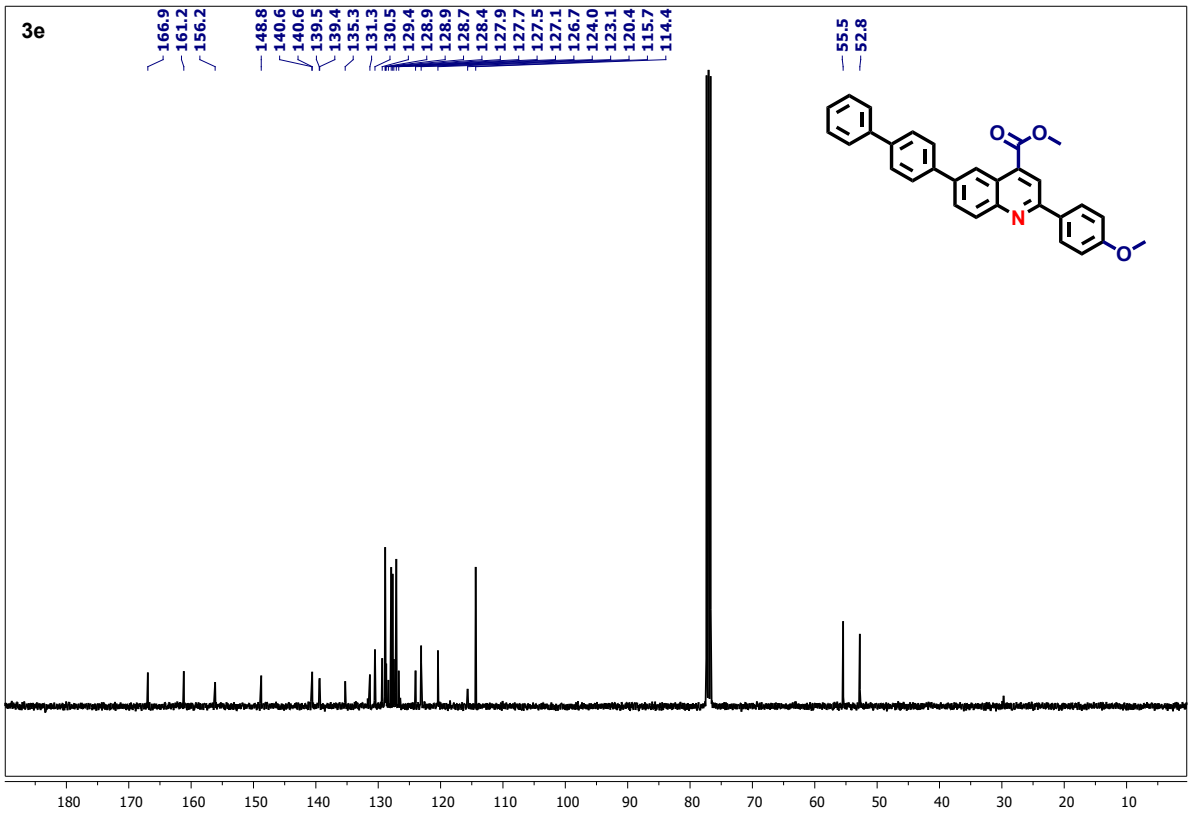

Figure S15. ^{1}H and ^{13}C NMR spectra of compound **3e**.

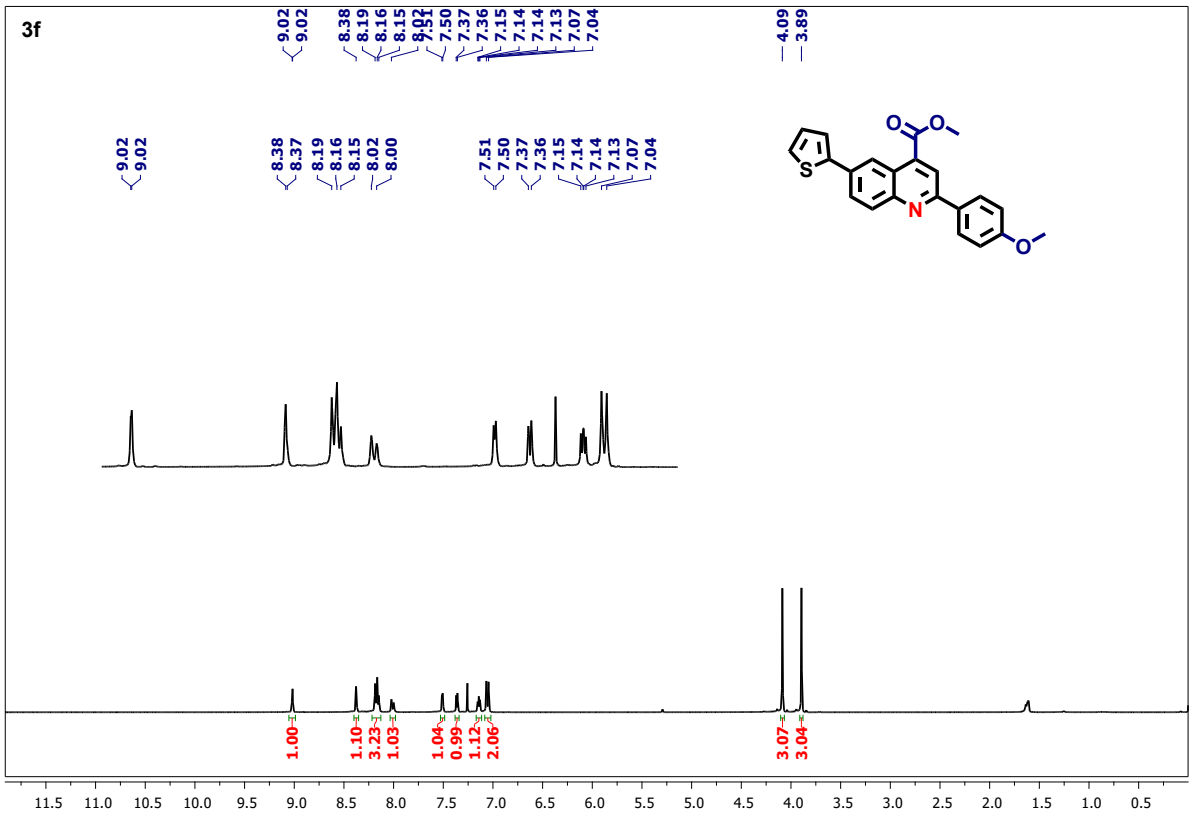

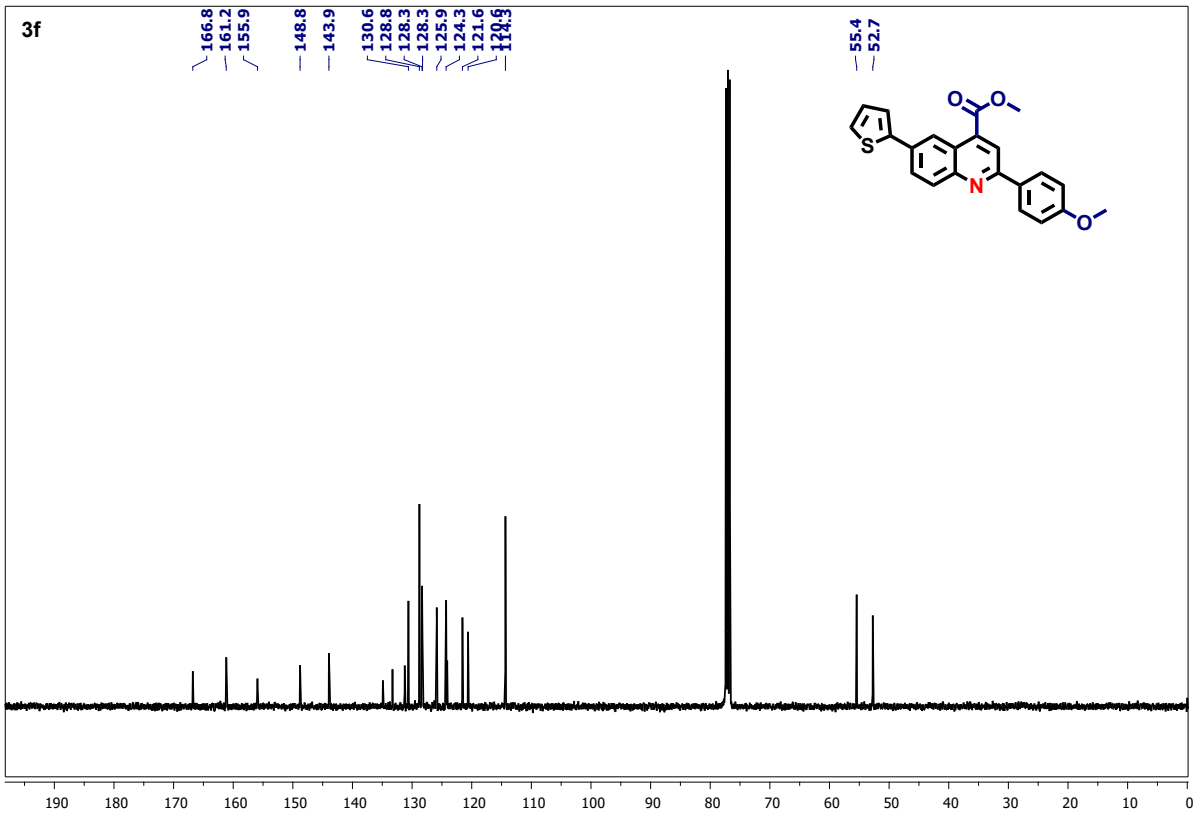

Figure S16. ^{1}H and ^{13}C NMR spectra of compound **3f**.

[i] W. Kern, Ed. Handbook of Semiconductor Cleaning Technology, Ch. 1.; Noyes Publishing: Park Ridge,NJ, 1993.

[ii] W. Kern, J. Vossen, *Thin Film Processes*, Ch. 1.; Academic Press: New York, 1978.

[iii] H.H. Choi, K. Cho, C.D. Frisbie, H. Sirringhaus, and V. Podzorov, *Nature materials*, 2018, **17**, 2-7.